Supplementary Information

Dopamine-integrated All-hydrogel Multi-electrode Arrays for Neural Activity Recording

Mingze Zeng[a], Jie Ding[a], Yuan Tian[a], Yusheng Zhang[a], Xiaoyin Liu[a,b], Zhihong Chen[a], Jing Sun[a], Chengheng Wu[a,c], Huabing Yin[d], Dan Wei[a]*, Hongsong Fan[a]*

[a] *National Engineering Research Center for Biomaterials, College of Biomedical Engineering, Sichuan University, Chengdu 610064, Sichuan, P. R. China*

[b] *Institute of Regulatory Science for Medical Devices, Sichuan University, Chengdu 610064, Sichuan, P. R. China*

[c] *Institute of Regulatory Science for Medical Devices, Sichuan University, Chengdu 610065, Sichuan, China*

[d] *James Watt School of Engineering, University of Glasgow, Glasgow G12 8LT, UK*

* Corresponding author email: Dan Wei (danwei@scu.edu.cn) and Hongsong Fan (hsfan@scu.edu.cn)

Experimental section

Ethical issues on animal experiments

All animal experiments in this study received approval from the Sichuan Provincial Laboratory Animal Management Committee (approval number: SYXK (Sichuan): 2019-189) and were conducted in accordance with the National Research Council's Guide for the Care and Use of Laboratory Animals.

Materials

PEDOT:PSS was purchased from Clevios (PH1000, Germany). The dopamine hydrochloride (DA·HCl), 1-(3-dimethylaminopropyl)-3-ethylcarbodiimide hydrochlorid (EDC), and N-hydroxysuccinimide (NHS) were purchased from Aladdin Co. Ltd. (Shanghai, China). Hyaluronic acid (HA, Mw = 700k~800k Da) was obtained from Bloomage Biotech. Co. Ltd. (Jinan, China). HRP (activity: 248 unit/mg) was obtained from TCI (Japan). Fluorescein diacetate (FDA) and propidium iodide (PI) was purchased from Sigma-Aldrich (USA). MXene was obtained from Beike (China). Unless otherwise stated, all other chemicals were acquired from Chengdu Kelong Chem. Co..

Sample Preparation

DA-treated PEDOT:PSS (PPD). PPD was synthesized by directly adding DA·HCl (10 mg) to PEDOT:PSS aqueous solution (10 mL, 10 mg/mL).[1] After stirring at room temperature (RT) for 30 mins, the product was obtained and stored at 4 °C for subsequent use. The successful synthesis of PPD was subsequently verified by 1H NMR spectrum (600 MHz, Bruker, USA).

Laser-treated PEDOT:PSS (LPP) and LPPD. A femtosecond lasers system (INNO Laser, China) that emitted a continuous-wave laser (532 nm) was used to selectively induce phase separation in PEDOT:PSS and PPD film, respectively. After that, the non-laser treated parts were removed by water-washing.

DA-modified hyaluronic acid (HAD) and MHD hydrogel. EDC (440 mg) and NHS (288 mg) were added to 10 wt% hyaluronic acid (HA) solution to activate the carboxy groups, followed by adding 0.47 g DA·HCl.[2] The reaction solution was stirred overnight at RT under nitrogen protection. The detected solution was then dialyzed for 3 days in deionized water (DIW) using a dialysis membrane (10,000 Da), and the pure product of HAD was obtained by freeze drying. To form a series of MHD hydrogels, 2.5 wt% HAD solution and MXene with various concentration (0, 1, 1.5 and 2 mg/mL, respectively) were mixed, followed by adding 30 μL of HRP solutions (1mg/mL) and 12.5 μL of H2O2 (0.5 mol/L).

Degummed silk fibroin (SF). The method of preparing degummed SF was reported in previous work.[3] In detail, 5 g

of silkworm cocoons was immersed in 2 L of 0.02 M Na2CO3 solution, and then boiled at 100 °C for half an hour. The product was rinsed with DIW to wash out the residual Na2CO3 solution. This process was repeated 3 times to obtain crude product. 2 g of the obtained product was added into 8 ml of 9.3 M LiBr solution and stirred for 4 h at 60 °C. Subsequently, the solution was dialyzed with DIW in an 8000 Da dialysis bag, followed by lyophilizing to obtain the degummed SF.

DA-modified SF (SFD). 5 mL of 8 wt% SF solution was placed in an ice bath, followed by adding 37.5 mg of EDC and 45 mg of NHS. After stirring for 30 min, 216 mg of DA·HCl was added to the solution.[4] Following a one-hour reaction, the mixture was dialyzed against DIW using a dialysis bag (14000 Da) for 3 days, and pure SFD was obtained by lyophilization. Following that, the products were examined using a 1H NMR spectrum (600 MHz, Bruker, USA).

Cross-linked SF (PSF) and SFD (PSFD) hydrogels. Polyethylene glycol diether (PEGDE, average Mn ~ 500) was added into 5 wt% SF or SFD solution, followed by a dynamic stirring at 60 °C heating. By pouring into a substrate, the solution formed a film after the water evaporation process in ambient air. After absorbing water, the PSF and PSFD films were converted to PSF and PSFD hydrogels. FT-IR (Nicolet IS5, ThermoFisher Scientific, USA) was then carried out to characterize the changes in the molecular structure of SF and SFD after the PEGDE-induced formation of films.[3]

Material characterizations

The content of PEDOT and PSS domain in PEDOT:PSS, PPD, LPP, and LPPD hydrogels was analyzed by XPS (AXIS SUPRA, Kratos, UK). The chemical structure of PEDOT chains in these groups was analyzed with Raman spectroscopy (inVia Raman microscope, Renishaw, UK). The AFM (Dimension Icon, Bruker, Germany) was used to characterize the phase separation of PEDOT and PSS. Electron spin resonance (ESR) test (JES X310, JOLE, Japan) was used to detected the radical character of these PEDOT:PSS-based materials.

Morphology characterizations

SEM (S-4800, Hitachi, Japan) was used to characterize the cross-section morphology of hydrogels and the interface between the conductive layer and the shielding layer at an acceleration voltage of 3.0 kV. TEM (JEOL, Japan, JEM 2100 F) was used to observe the single-layer structure of MXene.

Mechanical characterizations

For the tensile strength test of SF and PSFD hydrogels, a 100 μm thick film was made into a rectangular shape (5 mm × 20 mm), and then tested with a dynamic mechanical analyzer (DMA, TA Q-800, USA) at an extension speed

of 20 mm/min. Three parallel samples for each group were tested in relevant characterizations.

Electrical and electrochemical characterizations

Conductivity measurements were carried out by a four-point probe method with a semiconductor analyze system (ST2742B, Lattice Electronics, China), in which the interelectrode spacing (S) of each electrode was 1 mm. The conductivity (σ) is calculated by σ=1/(2πSV/I). V represents the potential difference between the second and third probe, and I represents the current running through first and fourth probe. At least five measurements were carried out for an average value. Cyclic voltammetry (CV) analysis of these PEDOT:PSS-based materials were carried out using an electrochemical workstation (Reference 600, Gamry Instruments, USA), where a silver/silver chloride (Ag/AgCl) was used as the reference electrode and PBS was used as the electrolyte.

Evaluation of impedance variations due to electrode deformation

Each individual electrode circuit was terminated and interfaced with a digital multimeter, where current fluctuations (I) were logged under a constant 3V voltage output (V). Subsequently, the corresponding impedance (R) values are derived using Ohm's Law expression of R = V/I.

Characterization of electromagnetic shielding performance

EMI SE values and electromagnetic parameters in the frequency range of 8.2−40.0 GHz were measured by the waveguide method using a vector network analyzer (VNA, Agilent PNA-N5234A). The samples tested with 25 mm thickness were cropped to rectangles of 22.86 mm × 10.16 mm, 15.90 mm × 8.03 mm, 10.95 mm × 4.50 mm, 7.15 mm × 3.60 mm for the measurement in frequency range of 8.2−12.4 GHz (X-band), 12.4−18 GHz (Ku-band), 18−26.5 GHz (K-band), and 6.5−40 GHz (Kaband), respectively. The SET, SER, and SEA were calculated by the recorded S-parameters, using power coefficients determined by the following formulae for A, R, and T:

(1) $R = |S_{11}|^2 = |S_{22}|^2$

(2) $T = |S_{12}|^2 = |S_{21}|^2$

(3) $A = 1 - R - T$

(4) $SE_T(dB) = 10\log(\frac{1}{T})$

(5) $SE_R(dB) = -10\log(1 - S_{11}^2) = -10\log(1 - S_{22}^2)$

(6) $SE_A(dB) = SE_T - SE_R$

At least three samples were tested for each group.

Biocompatibility evaluation

For in vitro biocompatibility, PC12 cells were added to a 24-well plate at a density of 10000 cells per well in order to conduct a biocompatibility evaluation. After the complete adhere of cells, the neural electrode was placed in the culture plate for 5-day culture. Cell viability was evaluated by FDA/PI staining and observed with a confocal laser scanning microscope (CLSM, Leica-TCSSP5, Germany). For in vivo biocompatibility, the neural electrode was implanted under the skull of SD rat (female), and a rigid device made of Ag probes encapsulated with polyimide substrates was also implanted as control. After 14 days of implantation, the postoperative rats' brains were excised, and they were preserved in 10% formalin for 24 hours before being stained with 4',6-diamidino-2-phenylindole (DAPI), neurofilament protein (NF), glial fibrillary acidic protein (GFAP), inducible nitric oxide synthase (iNOS) and Arginase 1 (Arg1).

ECoG signals monitoring

A multi-channel neural signal recording system (BlackRock, Cereplex Direct, USA) was used to capture the ECoG signals in an epileptic seizure SD rat's model induced by 4-AP. In order to record ECoG signals, the neural electrode was implanted in the primary visual cortex located at left hemispheres, and the reference electrode was concurrently attached to the dura mater of rats. The sampling rate was set to 1 kS/s, with bandpass filtered at 1~250 Hz and 40~100kHz for LFP and action potentials recording, respectively. The raw neural signals were further analyzed using a NeuroExplorer software.

Electrical neuromodulation

An isolated high-power stimulator (A-M systems, model 4100) was used to apply electrical neuromodulation. The LPPD10 hydrogel was implanted in the cerebral cortex and connected to the positive and negative terminals of the equipment via silver wires, respectively. A monophasic 100 mV pulse with a duration of 0.3 ms at a period of 100 ms was output for stimulation.

Statistical Analysis

Unless otherwise stated, all data are expressed as mean ± standard deviation (SD). The statistical analysis among the multiple groups was performed using one-way analysis of variance (ANOVA). Statistically significant was indicated by $*p < 0.05$, $**p < 0.01$, $***p < 0.001$, and $****p < 0.0001$.

Additional Results

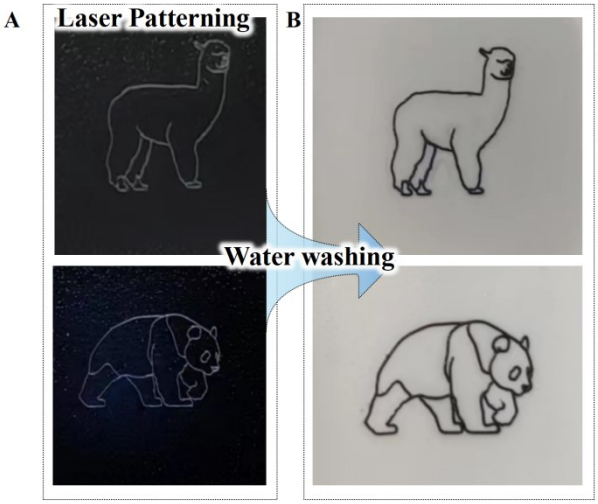

Figure S1. The images of formed PEDOT:PSS-based patterned hydrogel (A) before and (B) after water washing.

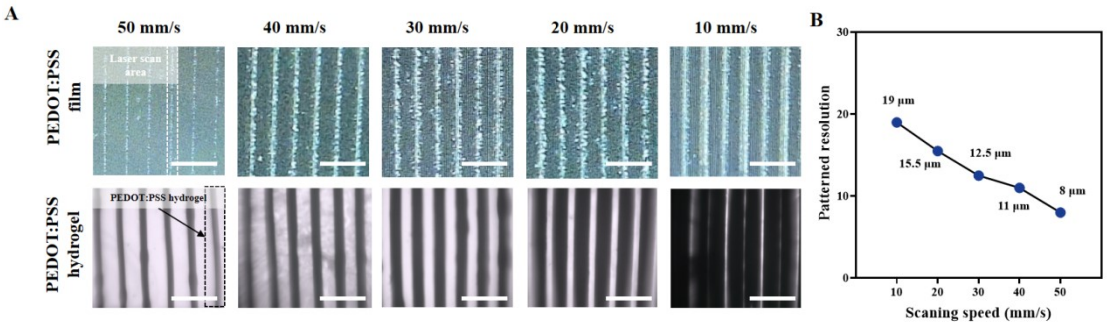

Figure S2. Effect of laser scanning speed on the resolution of patterned PEDOT: PSS hydrogels. (A) Images of PEDOT:PSS film (top, before washing) treated by laser with different scanning speed and the formed hydrogel (bottom, after washing) with various pattern resolutions. Scale bar: 50 μm. (B) Statistics on the resolution of patterned PEDOT:PSS hydrogels treated by different laser scanning speed.

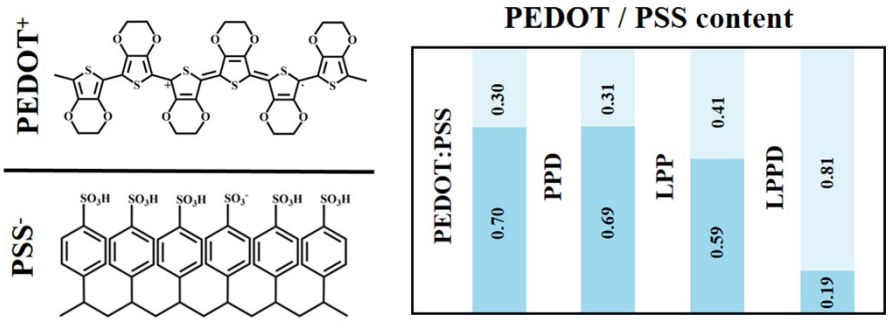

Figure S3. PEDOT/PSS ratios of PEDOT:PSS, PPD, LPP and LPPD.

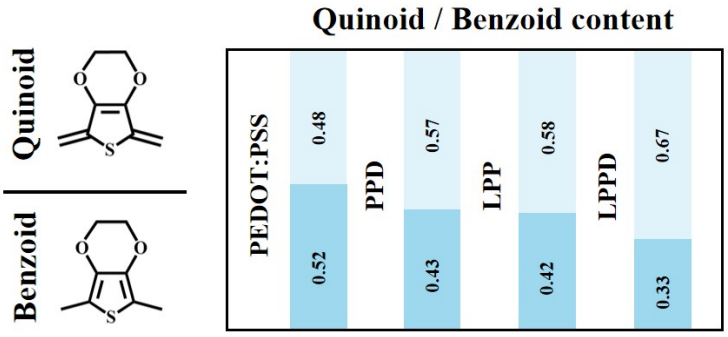

Figure S4. Quinoid/benzoid ratios of PEDOT:PSS, PPD, LPP and LPPD.

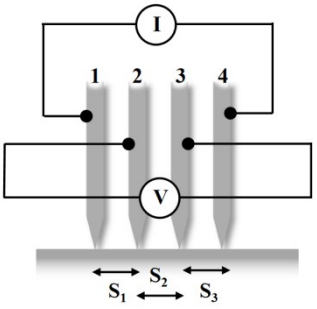

$$\sigma = \frac{I}{VC} \quad \text{(1)}$$

$$C = \frac{20\pi}{\frac{1}{S_1} + \frac{1}{S_2} - \frac{1}{S_1 + S_2} - \frac{1}{S_2 + S_3}} \quad \text{(2)}$$

Figure S5. Schematic diagram of four-point probe method for conductivity measurement and conductivity calculation formula.

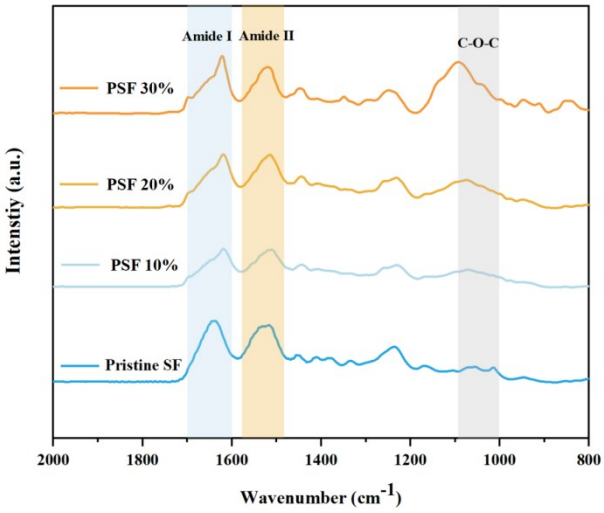

Figure S6. FTIR spectra of SF and PSF hydrogels treated with different weight ratios of PEGDE.

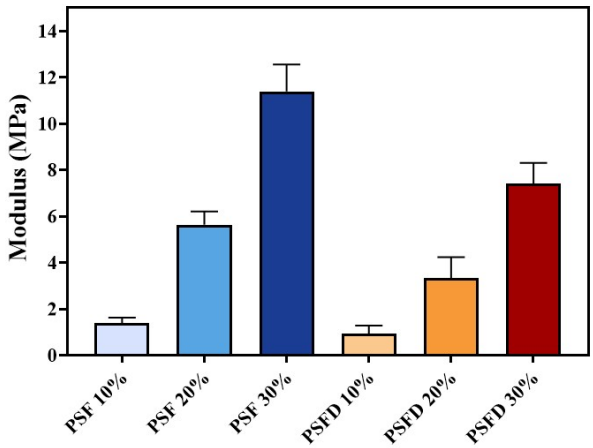

Figure S7. Modulus of PSF and PSFD hydrogels with different concentration of PEGDE under tensile mode.

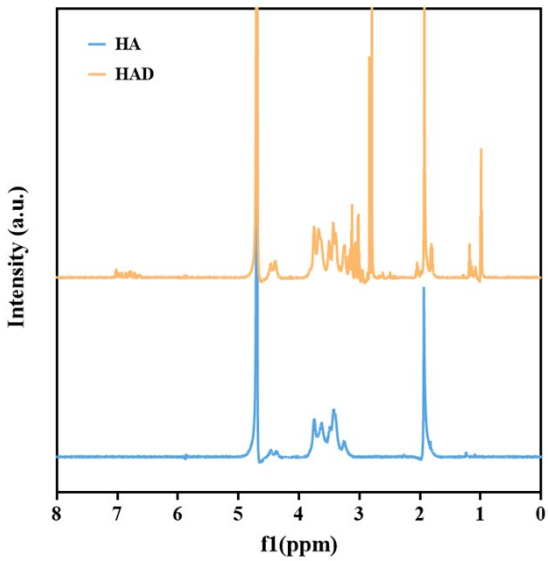

Figure S8. ^{1}HNMR spectra of HAD and HA.

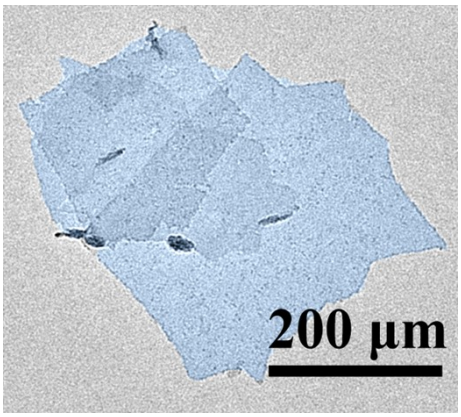

Figure S9. TEM image of MXene.

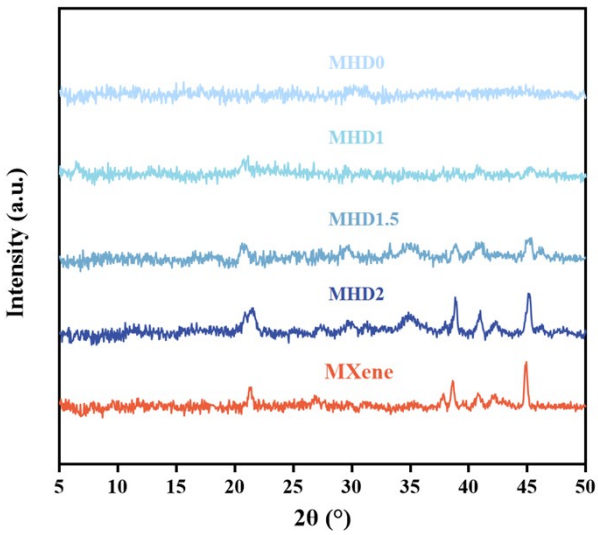

Figure S10. XRD spectra of MXene and MHD hydrogels with different concentration of MXene.

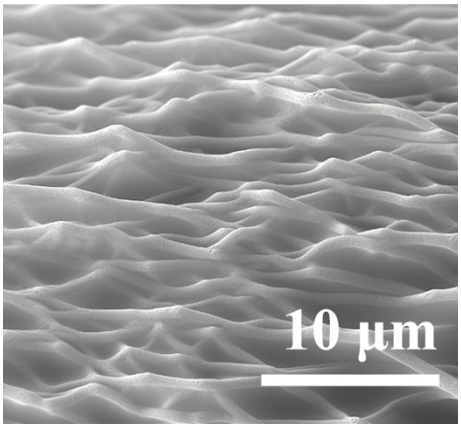

Figure S11. SEM image of MHD hydrogel.

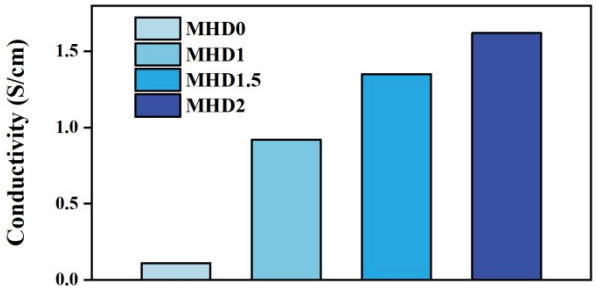

Figure S12. The conductivity of MHD hydrogels with different concentration of MXene.

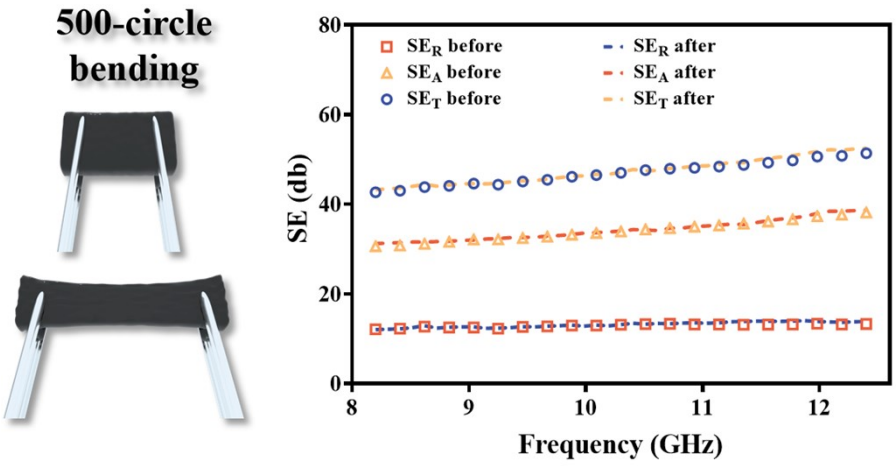

Figure S13. The X-band EMI SE of MHD2 hydrogel before and after 500-circle bending.

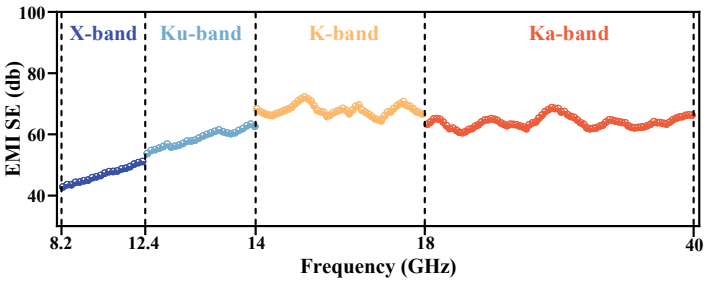

Figure S14. The X-band (8.2~12.4 GHz), Ku-band (12.4~14 GHz), K-band (14~18 GHz), and Ka-band (18~40 GHz) EMI SE of MHD2 hydrogel.

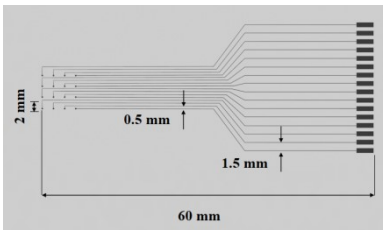

Figure S15. The parameter of 16-channel MEAs pattern.

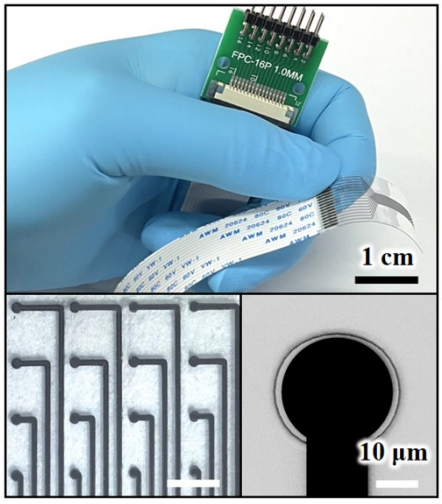

Figure S16. Picture showing the prepared neural electrode connected to a FPC (top). Arrangement of 16 individual electrodes and microscopic view of electrode exposure after laser etching (bottom).

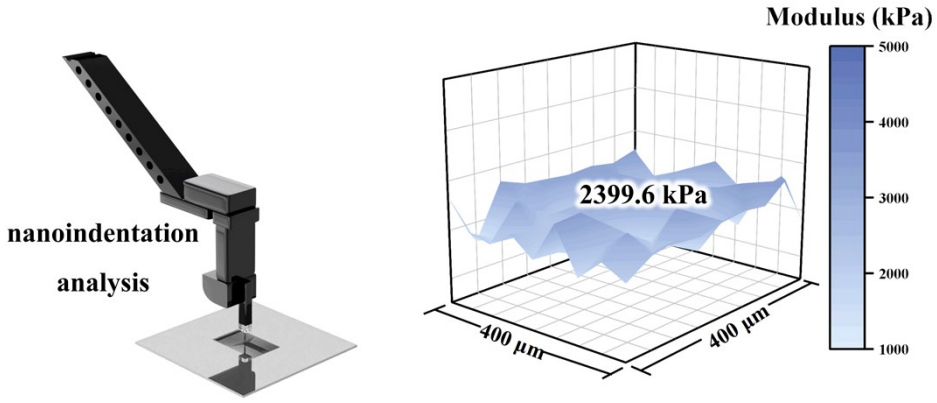

Figure S17. Nanoindentation analysis of Lap-shear test of all-hydrogel multi-electrode arrays.

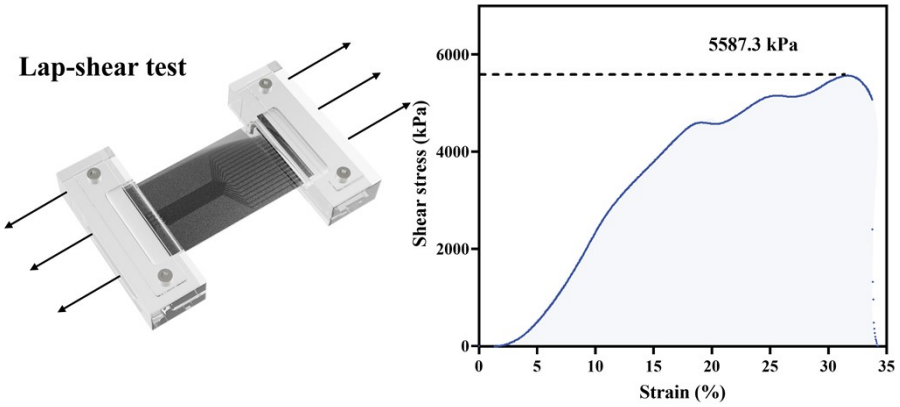

Figure S18. Lap-shear test of all-hydrogel multi-electrode arrays.

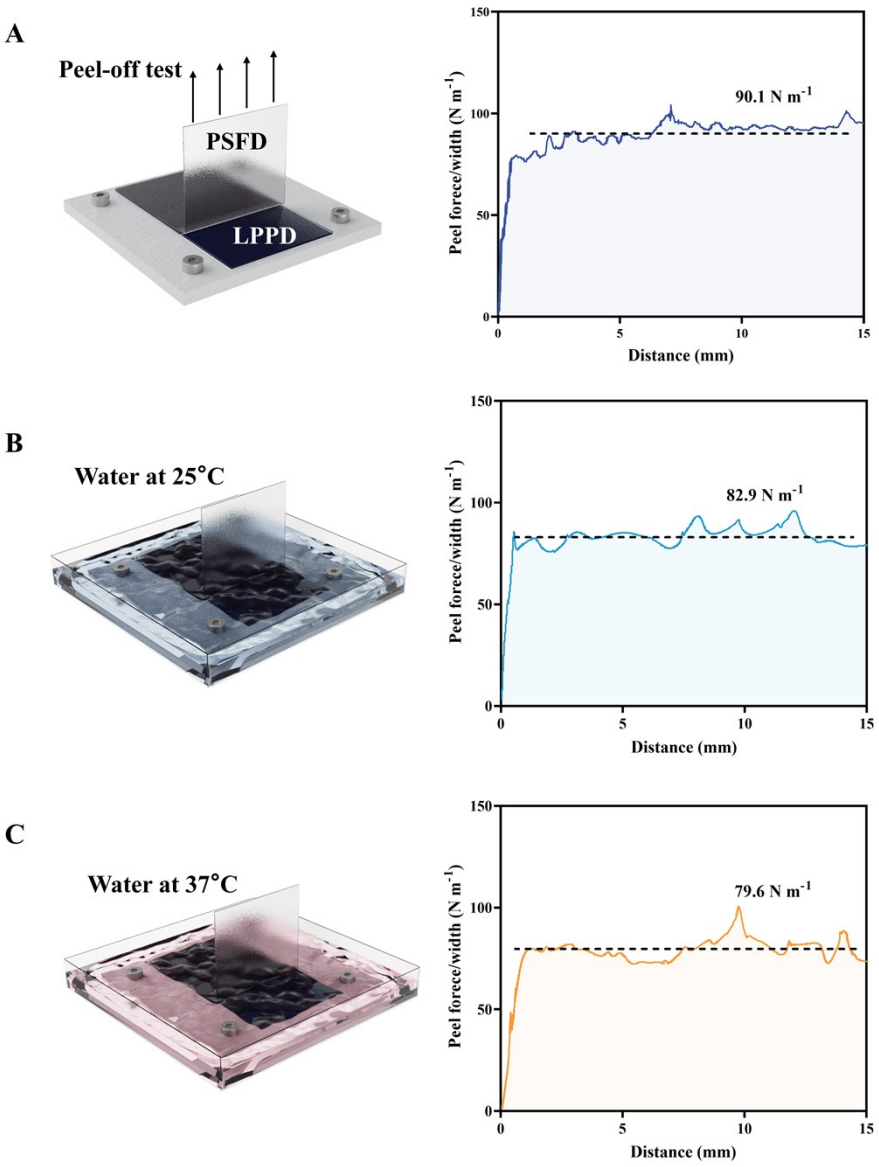

Figure 19. Peel-off tests of all-hydrogel multi-electrode arrays under different conditions.

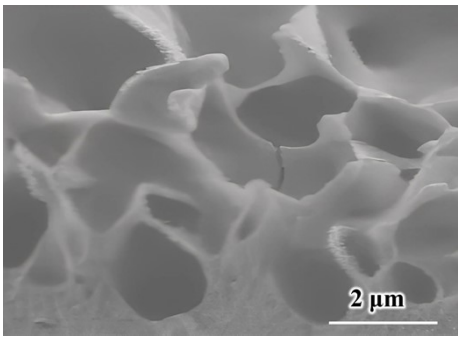

Figure 20. AFM phase images of PEDOT:PSS, PPD, LPP, and LPPD.

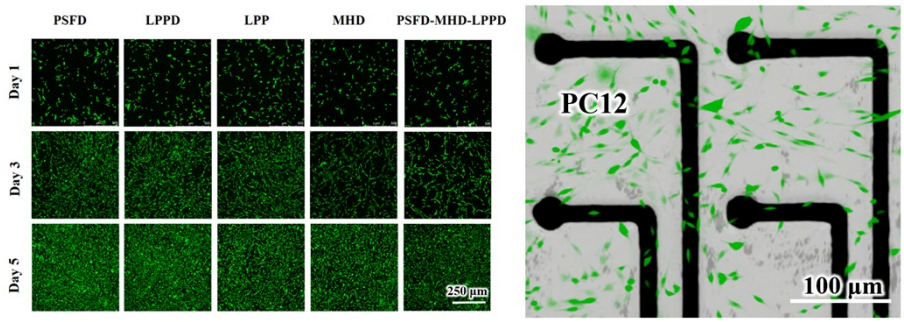

Figure S21. Live/Dead staining of PC12 co-cultured with different layer and an entire four-layer neural electrode. PSFD group means PC12 co-cultured with PSFD layer, LPPD group means PC12 co-cultured with LPPD layer. LPP group means PC12 co-cultured with LPP layer. MHD group means PC12 co-cultured with MHD layer. PSFD-MHD-LPPD group means PC12 co-cultured with a four-layer neural electrode consisted of MHD layer, PSFD, LPPD and PSFD layer.

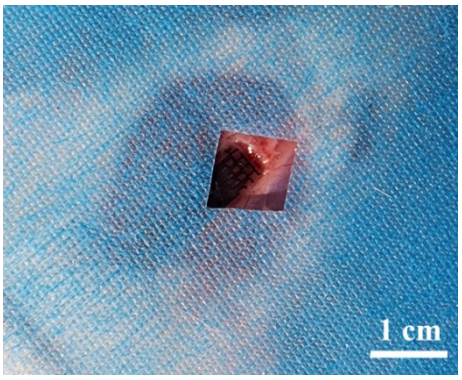

Figure S22. The location of this prepared all-hydrogel neural electrode in the brain of a rat.

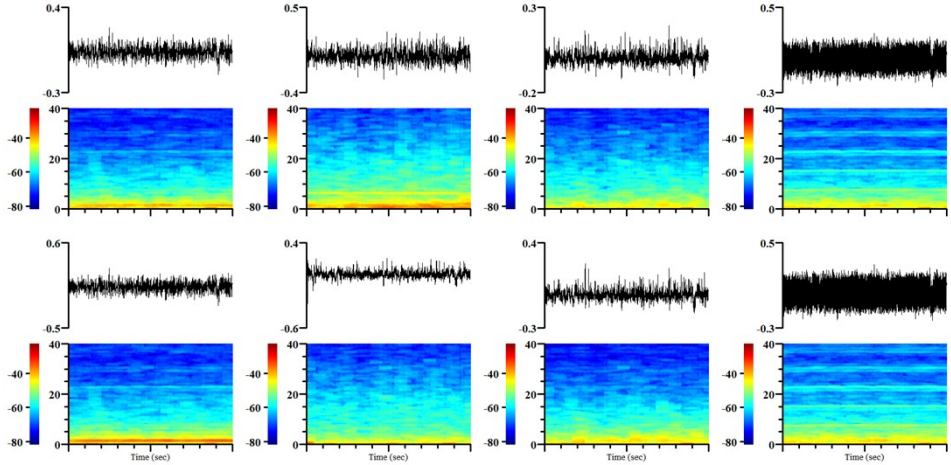

Figure S23. Representative multi-channel (channel 9-16) recorded LFP signals (top) and corresponding time-frequency spectrogram (bottom) of rest state in an epileptic rat.

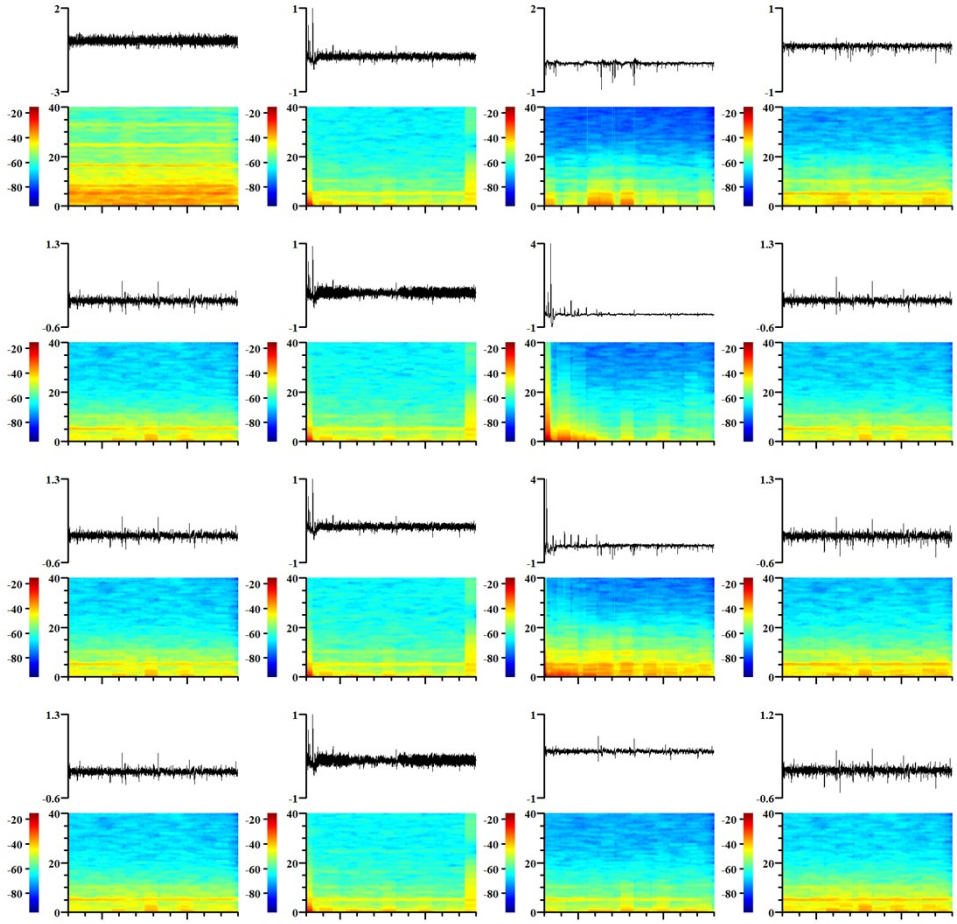

Figure S24. Representative multi-channel (channel 1-16) recorded LFP signals (top) and corresponding time-frequency spectrogram (bottom) of early epilepsy in an epileptic rat.

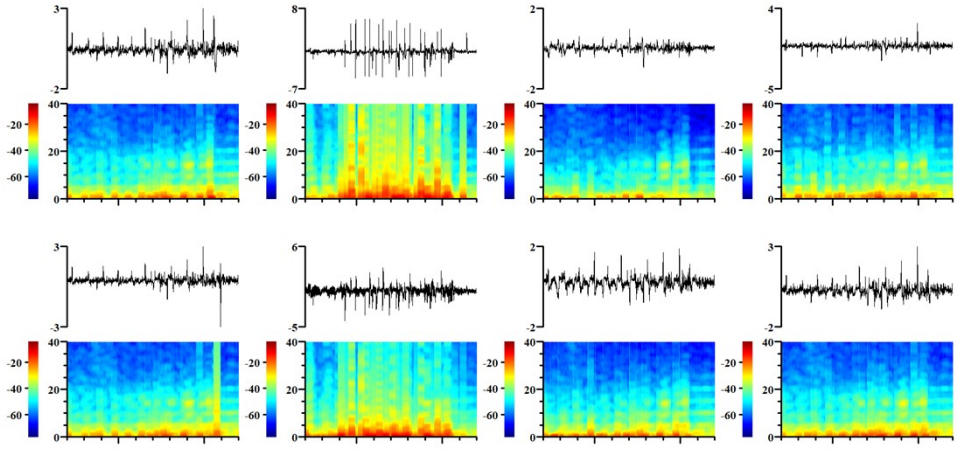

Figure S25. Representative multi-channel (channel 9-16) recorded LFP signals (top) and corresponding time-frequency spectrogram (bottom) of late epilepsy in an epileptic rat.

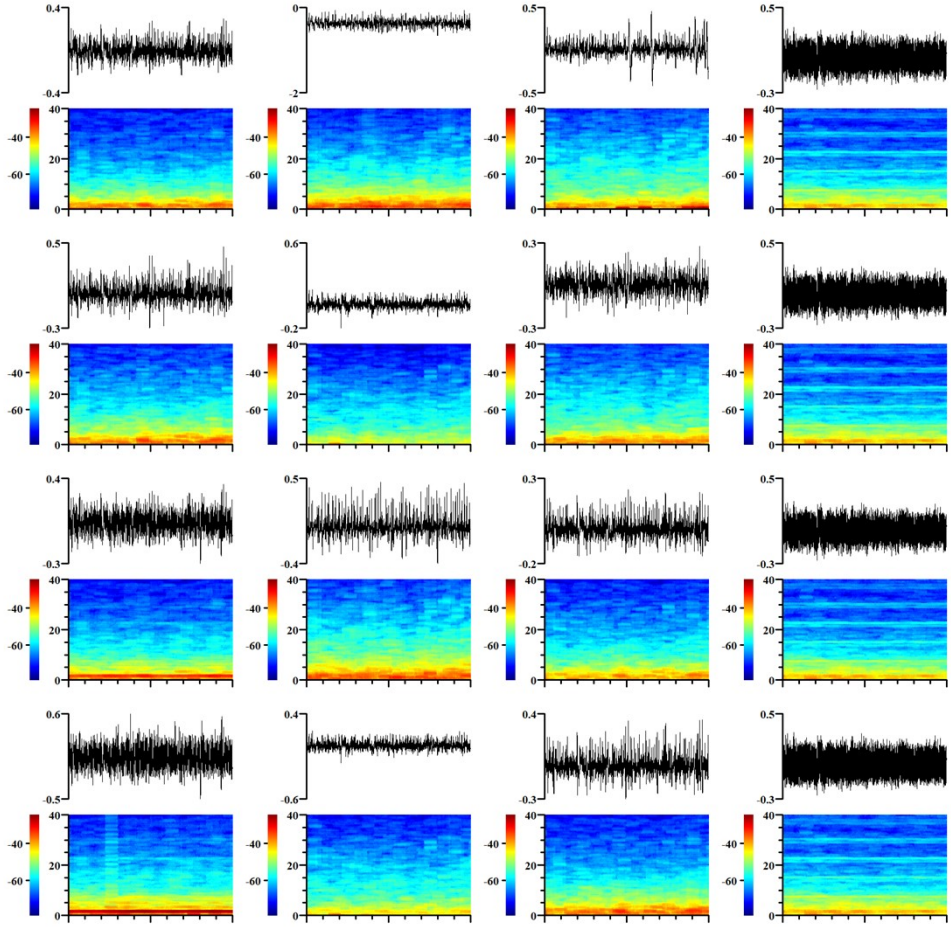

Figure S26. Representative multi-channel (channel 1-16) recorded LFP signals (top) and corresponding time-frequency spectrogram (bottom) of post recovery state in an epileptic rat.

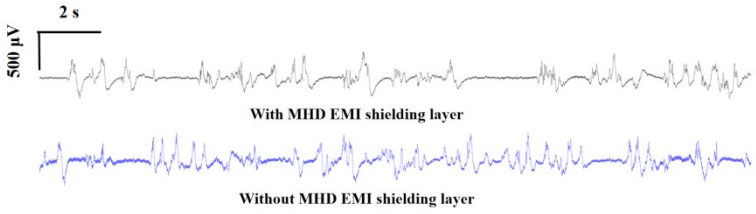

Figure S27. The reduction of background noise by EMI shielding layer. LFP recorded by a neural electrode with (top) and without (bottom) EMI shielding layer. After removing the electromagnetic shielding layer, the recorded background noise of LFP significantly increased.

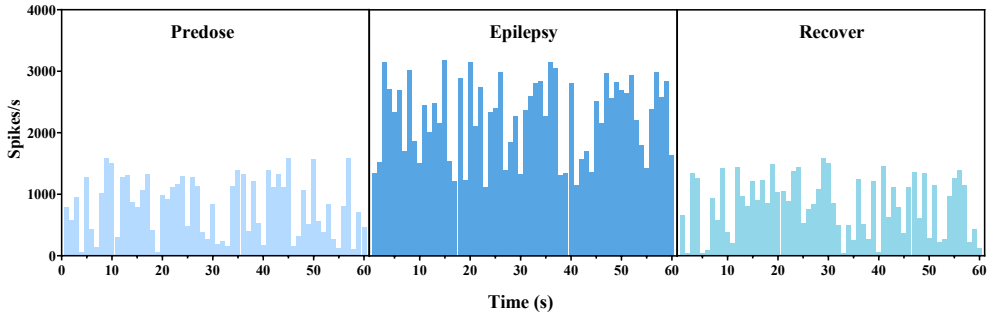

Figure S28. The total number of spikes recorded per second.

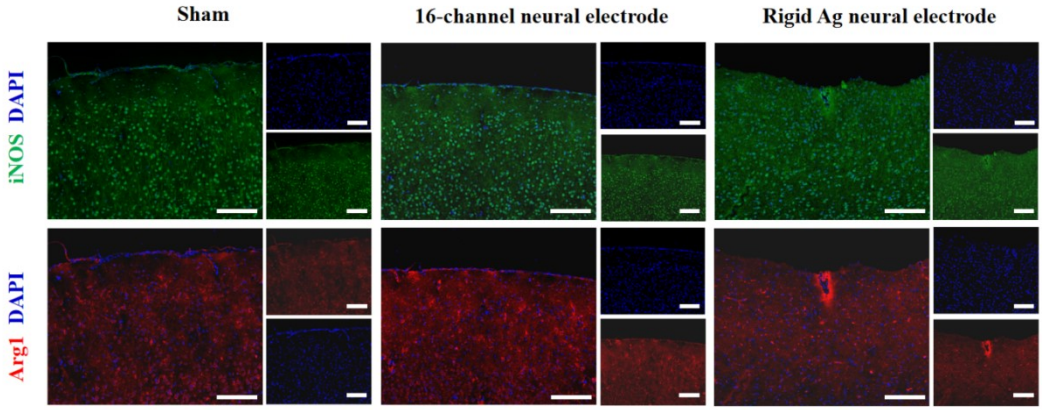

Figure S29. Immunofluorescence images of a brain slice after the insertion of a soft 16-channel all-hydrogel neural electrode and a rigid Ag neural electrode after 2 weeks. iNOS: inducible nitric oxide synthase, a maker of immune activation and inflammation. Arg1: arginase-1, a polarization marker of macrophages. Scale: 100 μm. The absence of any interaction between Ag electrode and substrate leads to direct separation of the electrode after implantation, as well as more aggressive macrophage aggregation and tissue damage.

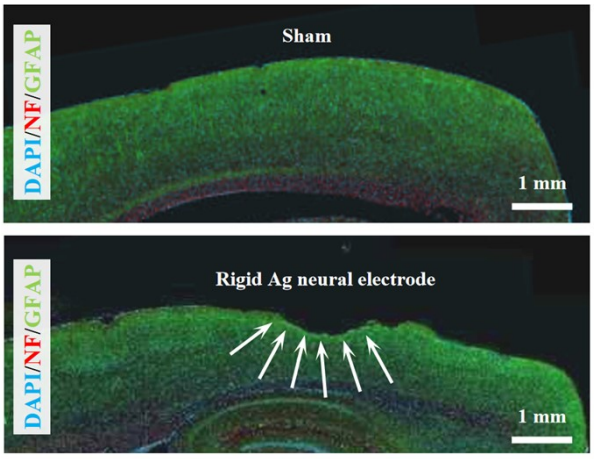

Figure S30. Immunofluorescence images of the rat's brain slices after the insertion of a rigid Ag neural electrode

after 2 weeks. A brain slice without the electrode implantation was used as control (sham group). NF: neurofilament, a marker of developing neurons. GFAP: glial fibrillary acidic protein, a glial maker.

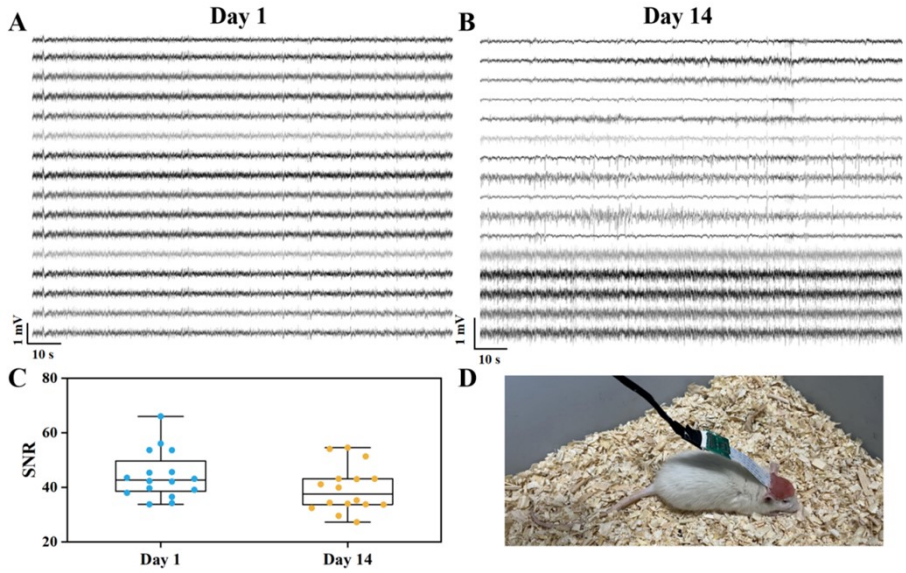

Figure S31. Recorded LFP from the surface of the cortex. (A) The recorded LFP signals on day 1 and (B) after 2 weeks of surgery. (C) SNRs of LFP signals obtained at day 1 and day 7, from the 16-channel all-hydrogel neural electrode. (D). Picture showing a free-moving rat with the 16-channel all-hydrogel neural electrode. The front end of the device is fixed by dental cement after implantation.

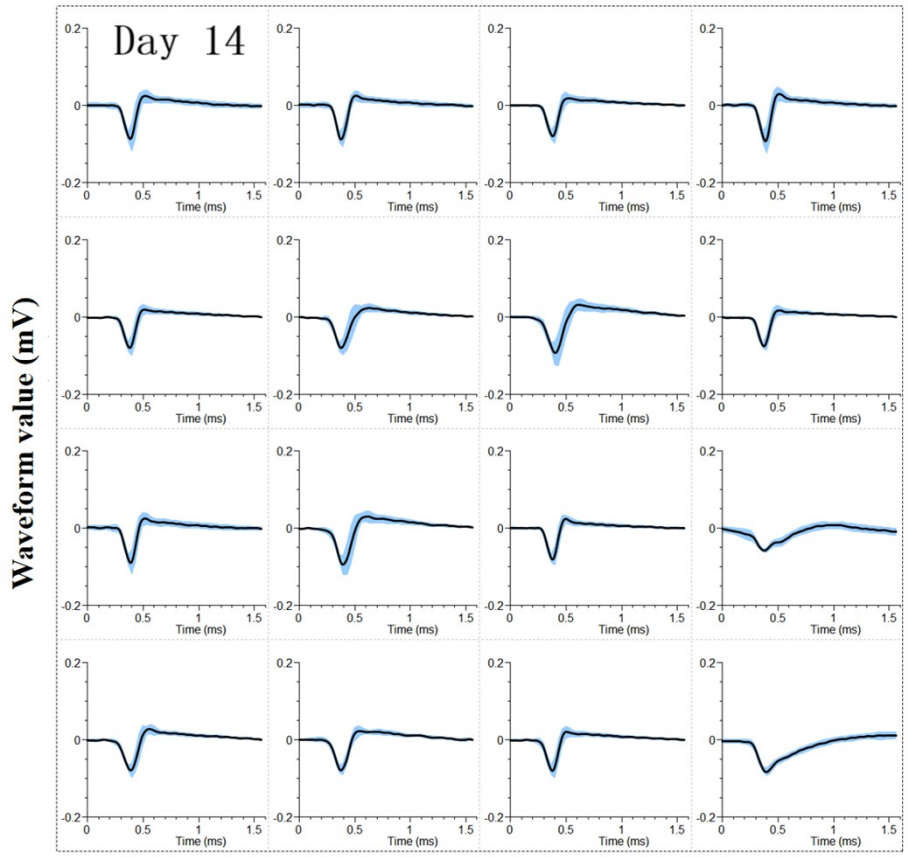

Figure S32. The 16-channel recorded spikes at 2 weeks after implantation.

Supplemented Table S1. Comparison of sensing capabilities of the reported pressure sensors

Ref.	**Journal**	**Method**	**Forms**	**Conductivity (S/cm)**
35	Journal of Electronic Materials	Glycerol doping and post-treatment	Film	1300
36	Energy & Environmental Science	Methanol doping and post-treatment	Film	1362
37	Journal of Applied Physics	Ethylene glycol doping and post-treatment	Film	1418
38	Advanced Functional	1-ethyl-3-methylimidazolium	Film	2084

	Materials	tetracyanoborate doping		
39	Advanced Electronic Materials	Nitric acid dipping	Film	4100
40	Advanced Materials	Fumed H2SO4 post-treatment	Film	4380
41	Nature Electronics	Laser processing method through a transparent substrate	Hydrogel	543
31	Nature Communications	Annealing after DMSO solvent replacement	Hydrogel	500
42	Journal of Materials Chemistry B	Heating after doping with ionic solution	Hydrogel	127
43	Nature Communications	Liquid-in-liquid printing	Hydrogel	301
_	This Work	DA doping/laser treatment	Hydrogel	4176

Reference

1 M. Zeng, X. Wang, R. Ma, W. Zhu, Y. Li, Z. Chen, J. Zhou, W. Li, T. Liu and Z. He, *Adv. Energy Mater.*, 2020, **10**, 2000743.

2 M. Zeng, D. Wei, J. Ding, Y. Tian, X. Wu, Z. Chen, C. Wu, J. Sun, H. Yin and H. Fan, *Carbohyd. Polym.*, 2023, **302**, 120403.

3 Y. Cui, F. Zhang, G. Chen, L. Yao, N. Zhang, Z. Liu, Q. Li, F. Zhang, Z. Cui and K. Zhang, Adv. Mater., 2021, **33**, 2100221.

4 Z. Yin, H. Liu, M. Lin, W. Xie, X. Yang and Y. Cai, *Biomed. Mater.*, 2021, **16**, 045025.